JGR Biogeosciences

RESEARCH ARTICLE
10.1029/2022JG007063

Peat Decomposition and Erosion Contribute to Pond Deepening in a Temperate Salt Marsh

Sheron Luk[1,2], Meagan J. Eagle[3], Giulio Mariotti[4,5], Kelsey Gosselin[6], Jonathan Sanderman[7], and Amanda C. Spivak[8]

[1]MIT-Woods Hole Oceanographic Institution Joint Program, Woods Hole, MA, USA, [2]Marine Chemistry and Geochemistry Department, Woods Hole Oceanographic Institution, Woods Hole, MA, USA, [3]Woods Hole Coastal and Marine Science Center, U.S. Geological Survey, Woods Hole, MA, USA, [4]Department of Oceanography and Coastal Sciences, Louisiana State University, Baton Rouge, LA, USA, [5]Center for Computation and Technology, Louisiana State University, Baton Rouge, LA, USA, [6]Interdepartmental Graduate Program in Marine Science, University of California Santa Barbara, Santa Barbara, CA, USA, [7]Woodwell Climate Research Center, Falmouth, MA, USA, [8]Department of Marine Sciences, University of Georgia, Athens, GA, USA

Abstract Salt marsh ponds expand and deepen over time, potentially reducing ecosystem carbon storage and resilience. The water filled volumes of ponds represent missing carbon due to prevented soil accumulation and removal by erosion and decomposition. Removal mechanisms have different implications as eroded carbon can be redistributed while decomposition results in loss. We constrained ponding effects on carbon dynamics in a New England marsh and determined whether expansion and deepening impact nearby soils by conducting geochemical characterizations of cores from three ponds and surrounding high marshes and models of wind-driven erosion. Radioisotope profiles demonstrate that ponds are not depositional environments and that contemporaneous marsh accretion represents prevented accumulation accounting for 32%–42% of the missing carbon. Erosion accounted for 0%–38% and was bracketed using radioisotope inventories and wind-driven resuspension models. Decomposition, calculated by difference, removes 22%–68%, and when normalized over pond lifespans, produces rates that agree with previous metabolism measurements. Pond surface soils contain new contributions from submerged primary producers and evidence of microbial alteration of underlying peat, as higher levels of detrital biomarkers and thermal stability indices, compared to the marsh. Below pond surface horizons, soil properties and organic matter composition were similar to the marsh, indicating that ponding effects are shallow. Soil bulk density, elemental content, and accretion rates were similar between marsh sites but different from ponds, suggesting that lateral effects are spatially confined. Consequently, ponds negatively impact ecosystem carbon storage but at current densities are not causing pervasive degradation of marshes in this system.

Plain Language Summary Ponds are natural features of salt marshes but their expansion may be an indicator of ecosystem deterioration because they impede the marsh's ability to keep pace with sea-level rise and remove decades of buried soil carbon. The water filled holes created by ponds represent volumes of marsh soil carbon that are missing due to prevented accumulation or lost through erosion and decomposition. These loss pathways have different implications for coastal carbon cycling as eroded soils can be redeposited elsewhere while microbial decomposition represents permanent loss. We used geochemical and modeling approaches to assess how much of the carbon missing from ponds can be attributed to prevented soil accumulation, erosion, and decomposition as well as whether ponds reduce the integrity of the surrounding marsh. We estimate that these processes represent 32%–42%, 0%–38%, and 22%–68%, respectively, of soil carbon missing from three ponds in a New England salt marsh. The range of potential erosion losses reflect differences in fetch and wind-driven waves used in the models. Decomposition was calculated by subtracting the contributions of prevented accretion and erosion from the volume of missing carbon and, while the range is large, losses normalized over time are comparable to previously measured respiration rates. Comparisons of soil properties and composition between the ponds and surrounding marsh demonstrate that the effects of expansion are confined to within a 10 m perimeter. Consequently, in this system, ponds represent net losses from the carbon budget and at current densities are not causing pervasive degradation of the marsh.

Key Points:

- Salt marsh ponds deepen and expand over time but their effects are localized and do not result in deterioration of the surrounding marsh
- Three processes account for soil carbon missing from deepening ponds: prevented deposition, erosion, and decomposition
- Eroded soils may be redistributed and retained within the marsh, while decomposition represents carbon loss

Supporting Information:

Supporting Information may be found in the online version of this article.

Correspondence to:

A. C. Spivak,
aspivak@uga.edu

Citation:

Luk, S., Eagle, M. J., Mariotti, G., Gosselin, K., Sanderman, J., & Spivak, A. C. (2023). Peat decomposition and erosion contribute to pond deepening in a temperate salt marsh. *Journal of Geophysical Research: Biogeosciences*, *128*, e2022JG007063. https://doi.org/10.1029/2022JG007063

Received 18 JUL 2022
Accepted 23 JAN 2023

Author Contributions:

Conceptualization: Amanda C. Spivak
Funding acquisition: Amanda C. Spivak
Investigation: Amanda C. Spivak
Methodology: Sheron Luk, Meagan J. Eagle, Giulio Mariotti, Kelsey Gosselin, Amanda C. Spivak
Project Administration: Amanda C. Spivak
Validation: Amanda C. Spivak
Writing – original draft: Sheron Luk
Writing – review & editing: Meagan J. Eagle, Giulio Mariotti, Kelsey Gosselin, Jonathan Sanderman, Amanda C. Spivak

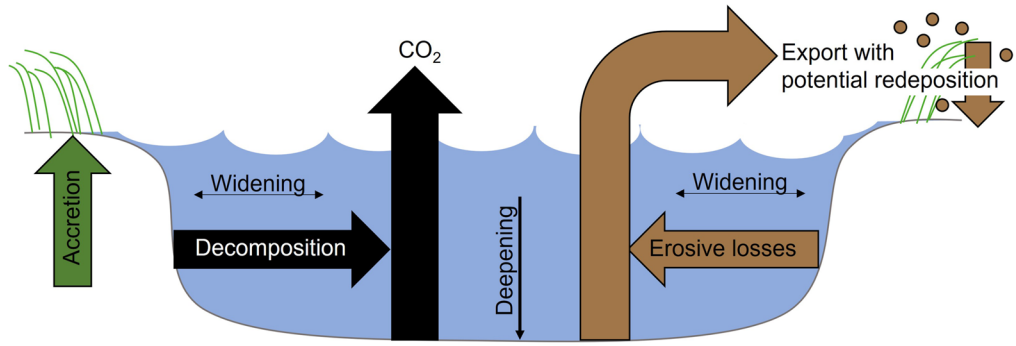

Process	Contributes to…	Assessed by…
Marsh accretion	Pond deepening by way of marsh elevation gain	Developing marsh vertical accretion models through radiometric dating.
Erosive losses	Pond deepening and widening	Modeling wind-driven resuspension and export. Comparing soil radioisotope inventories.
Decomposition	Pond deepening and widening	Soil bulk property characterization, organic matter thermal indices, lipid biomarker proxies of organic matter sources and reactivity. Prior studies of whole-pond metabolism rates (Spivak et al. 2017, 2018, 2020)

Figure 1. Three main processes contribute to pond deepening and expansion. Vertical accretion of the surrounding marsh platform (green) contributes to relative pond deepening because ponds are not depositional environments. Wind-generated waves cause soil erosion and export (brown) through benthic resuspension and pond edge retreat. Exported soils may be redeposited on the marsh surface, contributing to vertical accretion, or washed into adjacent coastal waterways. Decomposition (black) along pond walls and bottoms results in permanent organic matter loss as carbon dioxide (CO_2) or dissolved inorganic carbon. We predict that erosive losses are more important during early phases of pond development while decomposition plays a progressively larger role over time. Contributions from accretion are constant over time, assuming a stable relationship between sea level and marsh position in the tidal frame over the past 100 years when acceleration of sea level rise was within sediment accretion uncertainty. The bottom table describes how the processes contribute to pond expansion and the analytical or modeling approaches we used to evaluate each.

1. Introduction

Disturbances to salt marsh ecosystems have the potential to alter important functions and delivery of valuable services (Barbier et al., 2011; Craft et al., 2009). Fast rising sea levels and management techniques that reduce soil drainage can catalyze the conversion of vegetated marsh into open water environments (Boston, 1983; DeLaune et al., 1994; Mariotti, 2016). Expansion and deepening of open water areas, also called ponds or pools, are often attributed to soil erosion and decomposition but the contributions of each process and how they change over time are open questions (Johnston et al., 2003; Ortiz et al., 2017; Turner & Rao, 1990). The implications of these processes differ as eroded soils can be redistributed across the marsh or exported to coastal waters while decomposition represents permanent loss of organic carbon (Figure 1). The combined effects of erosion and decomposition on pond deepening and widening may impact marsh sustainability by preventing future soilbuilding and reducing the integrity of the underlying and surrounding soils. Assessing the processes contributing to expansion is therefore key in understanding how ponds affect ecosystem soil dynamics and carbon storage.

Ponds have a dynamic life cycle whereby they can exist for decades before intersecting with a tidal creek, draining, and infilling through sediment trapping and re-establishment of emergent vegetation (Mariotti et al., 2020; Wilson et al., 2014). In some systems, pond formation and infilling are largely balanced (Smith & Pellew, 2021) while in others expansion leads to permanent marsh loss (Mariotti, 2016; Mariotti & Fagherazzi, 2013). Soil waterlogging in the marsh interior can lead to sulfide accumulation, grass dieback, and pond formation (Burdick & Mendelssohn, 1990; Mendelssohn & McKee, 1988). Death and collapse of marsh grass roots can result in >10 cm of elevation loss during early phases of pond formation, but this is difficult to quantify (Day et al., 2011; DeLaune et al., 1994). Ponds become decomposition hotspots with high soil respiration rates fueled by carbon from benthic microalgae and the underlying peat (Spivak et al., 2018). As a result, some ponds are net heterotrophic, meaning that more organic matter is respired than produced in situ (Johnston et al., 2003; Spivak et al., 2017, 2020). Scaling metabolism rates over pond lifespans suggests that decomposition could be responsible

for most—if not all—of the carbon lost during formation and deepening, after accounting for accretion of the surrounding marsh (Figure 1; Johnston et al., 2003; Spivak et al., 2017, 2020). However, extrapolating rates measured over days-to-seasons to timescales of years-to-decades has important caveats.

Wind-generated waves are the primary driver of erosion in ponds as they cause edge retreat and soil resuspension (Kearney et al., 1988; Mariotti, 2016; Ortiz et al., 2017; Stevenson et al., 1985). Consistent wind directions and storm paths can focus edge erosion such that ponds elongate along the same path (Ortiz et al., 2017; Stevenson et al., 1985). Lateral expansion of large ponds can accelerate over time as greater fetch distances facilitate faster erosion. Such runaway expansion may eventually result in the loss of large areas of vegetated marsh (Mariotti, 2016; Mariotti & Fagherazzi, 2013). Eroded soils can be exported to coastal waters and lost from the system or redeposited on the marsh and contribute to vertical accretion (Figure 1; Hopkinson et al., 2018; Luk et al., 2021). Resuspension may also facilitate organic carbon loss via decomposition, by moving particles from anoxic pond soils into oxic surface waters. However, since ponds can be nearly a meter deep (Adamowicz & Roman, 2005)—and hence lower than the wave base—other processes must also contribute to the loss of soil organic matter.

Geochemical signals in soils can provide insight into the effects of erosion and decomposition which alter both the physical structure (e.g., bulk density) and organic matter composition (e.g., lipid biomarkers; Figure 1). For instance, bulk density may decrease as decomposition removes organic matter and water fills pore spaces, while low radioisotope inventories (e.g., ^{210}Pb, ^{137}Cs) can point to erosional losses (DeLaune et al., 1994). Thermochemical properties provide an index of organic matter stability but hold limited information about carbon sources and transformations (Luk et al., 2021; Sanderman & Grandy, 2019; Williams & Plante, 2018). Complementary lipid biomarker analyses can be used to assess new organic matter inputs and degradation of older material as these compounds have high source fidelity and span a range of chemical reactivity (Canuel et al., 2007; Spivak et al., 2007). Two lipid classes, fatty acids (FA) and hydrocarbons, are particularly useful as they represent relatively fresher and more detrital organic matter, respectively (Canuel et al., 1997; Spivak, 2015; Wang et al., 2003). Because these proxies hold different information overlaying them provides a more holistic assessment of the processes changing soil structure and composition.

The water-filled volumes of ponds represent carbon stocks missing from the marsh. We evaluated how three processes account for the missing carbon: avoided accretion, decomposition, and erosion (Figure 1). Avoided accretion was determined by developing soil age models from radioisotope (^{210}Pb) profiles of marshes and ponds and comparing inventories. We developed models of wind-driven waves to estimate potential erosional losses. Decomposition signals were assessed using multiple geochemical characterization approaches. We then estimated the net effect of ponds on the soil carbon inventory of a New England marsh. To determine whether pond expansion causes deterioration of the marsh, soil properties were compared at two distances from pond perimeters. Because ponds expand laterally and deepen over time, we expected that marsh soils adjacent to and underlying ponds would show signs of deterioration, but these would likely be spatially limited and not propagate far into the surrounding marsh.

2. Methods

2.1. Study Location and Sample Collections

We focused on three ponds and the surrounding high marshes within the Plum Island Ecosystems—Long Term Ecological Research (PIE-LTER) project domain (Figure 2a; 1.41–1.51 m North American Vertical Datum of 1988 [NAVD 88]). Emergent grass communities of *Spartina patens*, *S. alterniflora*, and *Distichlis spicata* surround the ponds which formed around the same time (1965–1978), are permanently inundated, and have similar depths (0.24–0.30 m), but different volumes, aquatic plant communities, and surface water and sediment metabolic rates (Spivak et al., 2017, 2018, 2020). The ponds are typical of those in the high marshes of PIE-LTER (Spivak et al., 2020) and were chosen because we wanted to assess whether erosive and decomposition effects were similar across ponds with different characteristics. At each of the three sites, we collected one pond core (60 cm) and two marsh cores (90 cm) that were 10–12 m (core M1) and 20–29 m (core M2) away. Sampling distances reflected the goals of capturing spatial gradients that were beyond the immediate perimeter of mudflats and sparse emergent grasses but reflect zones with potentially greater (M1) or lesser (M2) pond influence (e.g., transitions from *S. alterniflora* to *D. spicata*) and were at a spatial resolution relevant to marsh models. Limited

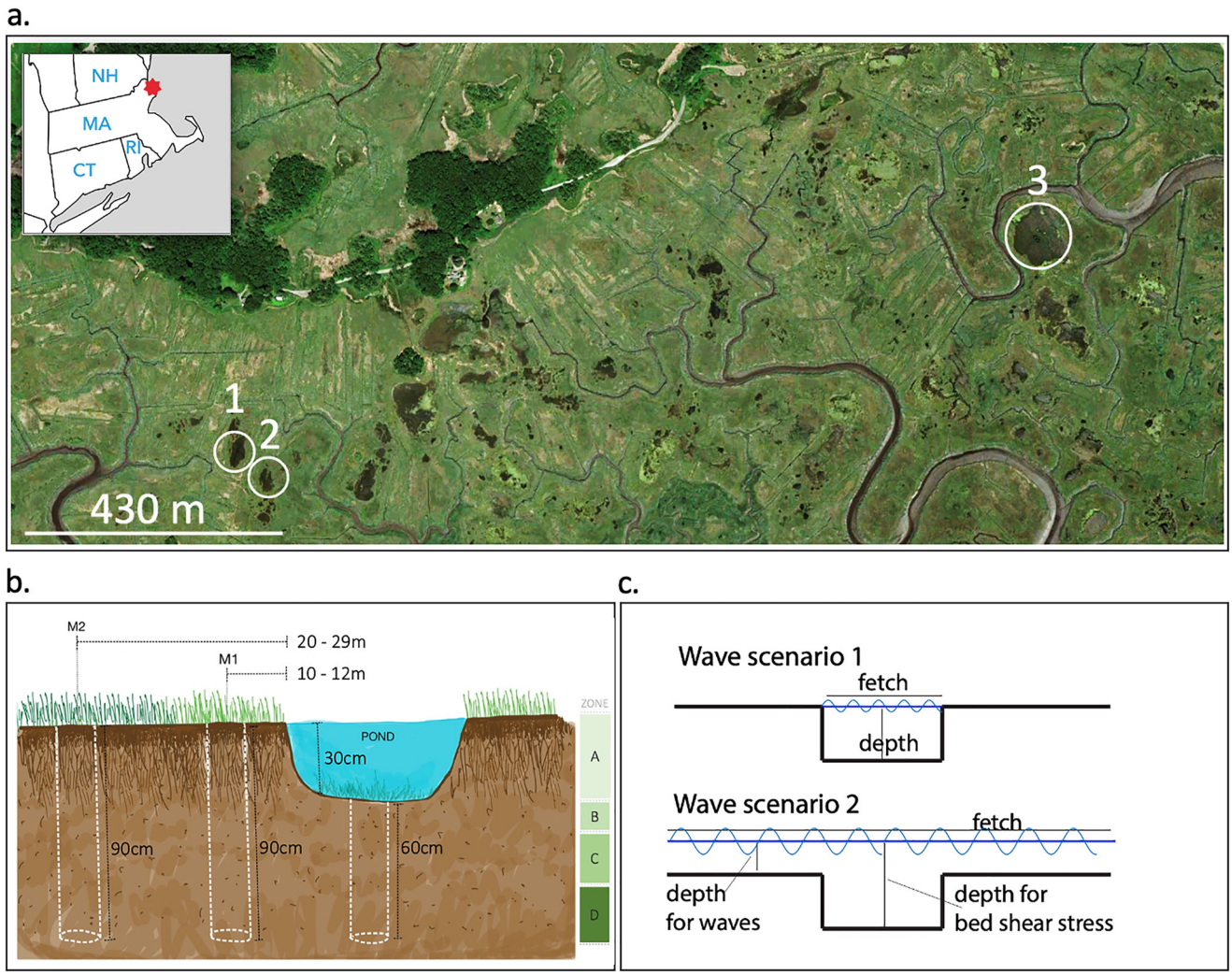

Figure 2. (a) Location of the three ponds on the high marsh platform of Plum Island Ecosystems—Long Term Ecological Research site (MA, USA) (aerial imagery: Google, 2022). (b) Soil cores were collected from ponds and nearby (M1) or farther away (M2) sites in the emergent marsh. Comparisons between overlapping horizons between the ponds (0–60 cm) and marsh (30–90 cm) were used to evaluate processes contributing to pond deepening. Soil zones are defined as (A) marsh surface soils and emergent grass rooting zone, (B) pond upper soils, (C) intermediate, and (D) deeper horizons. (c) Wind-driven erosion was modeled based on two scenarios of fetch and water depth: one for tidally isolated ponds (top) and a second for when high tides inundate the marsh platform (bottom).

sample replication within and between ponds reflects a tradeoff between high-resolution down-core profiles needed to assess erosion and decomposition effects with resource intensive geochemical analyses while lateral sampling distances were physically constrained by tidal channels and mosquito ditches.

In summer—fall 2014, we conducted elevation surveys, characterized pond biogeochemistry and metabolism rates, and collected soil cores (Luk et al., 2021; Spivak et al., 2017, 2018). This study builds on our previous work by using multiple geochemical proxies to assess erosion and decomposition signals in ponds and whether they propagated laterally into the marsh, and by estimating wave-driven resuspension and erosion. Elevation was measured with a Real Time Kinematic – Global Positioning System and was similar at the M1 (1.45 ± 0.02 m NAVD 88) and M2 (1.45 ± 0.03 m NAVD 88) sites. Pond depths were measured with a meter stick and referenced to elevation at the edges. Soil cores were collected in large diameter barrels and compaction was not observed upon retrieval (10 cm diameter × 60–90 cm long). The cores were refrigerated until processing within 1–2 days, when they were split lengthwise with one half sectioned at 1–2 cm intervals (bulk properties, elemental composition, radioisotope activities) and the other half at 2–5 cm intervals (organic matter composition), with greater resolution (2 cm) in surface horizons (top 30 cm). Sampling resolutions reflected our expectation that structural and compositional changes associated with decomposition would be concentrated in pond surface horizons

(0–10 cm) and that any lateral ponding effects would be evident in marsh horizons that overlapped with pond surface waters (i.e., 0–30 cm).

2.2. Bulk Soil Properties and Elemental Composition

Soil bulk density (g cm^{-3}) was determined gravimetrically by drying to constant mass (60°C). Soils were sieved (<1 mm) to remove large roots, leaving the fine fraction representing refractory soil organic carbon (SOC). In preparation for elemental and isotopic analysis, samples were homogenized with a Retsch Mixer Mill 200. Approximately 90% of samples were fumed with 12 N hydrochloric (HCl) acid to remove inorganic carbonates (Hedges & Stern, 1984; Lorrain et al., 2003) and subsequently analyzed for total organic carbon (TOC), total nitrogen, and stable isotope composition ($\delta^{13}C$, $\delta^{15}N$; ‰) at the Stable Isotope Laboratory at the Marine Biological Laboratory (Woods Hole, MA) using a Europa ANCA-SL elemental analyzer-gas chromatograph preparation system interfaced with a continuous-flow Europa 20-20 gas source stable isotope ratio mass spectrometer. Carbon content of the remaining samples was estimated using Fourier transform infrared (FTIR) spectroscopy from a Thermo Nicolet 6,700 FTIR spectrometer equipped with a Pike AutoDiff automated diffuse reflectance accessory (Sanderman et al., 2015) and partial least squares regressions (Janik et al., 2007; Luk et al., 2021). We focused on the far marsh cores (M2) because we expected a stronger contrast against pond soils. Marsh surface and rooting zone soils (0–30 cm) were analyzed at a 10 cm resolution while overlapping marsh and pond horizons were analyzed at a 4–6 cm resolution, reflecting the tradeoff between needed down core resolution and analytical resources.

2.3. Thermal Reactivity

We assessed the thermal reactivity of SOC using ramped pyrolysis oxidation (RPO) at the National Ocean Sciences Accelerator Mass Spectrometry Facility (Woods Hole MA; Luk et al., 2021). Selected horizons from the M2 and pond cores captured the marsh surface (0 cm marsh; 1.41–1.50 m NAVD 88), pond surface (~30 cm marsh; 0 cm pond; 1.14–1.20 m NAVD 88), and deeper horizons (~80 cm marsh; ~50 cm pond, 0.66–0.73 m NAVD 88). Homogenized samples were placed in a reactor where temperatures ramped from ambient to 1,000°C under a constant flow of ultra-high purity helium and oxygen to promote thermal degradation and oxidation of SOC (20°C min^{-1}; Rosenheim et al., 2008). The evolved carbon dioxide (CO_2) was measured using an infrared gas analyzer. We used the temperature at which 50% of CO_2 evolved (t50) as a proxy of thermal reactivity.

2.4. Lipid Biomarkers

We further assessed SOC composition by characterizing source-specific biomarkers in the ponds and far marsh sites (M2). We focused on two classes of biomarkers, FA and hydrocarbons, as they provide complementary source information and represent fresher and more detrital material, respectively (Bianchi & Canuel, 2011). Lipid biomarkers were extracted using a modified Bligh and Dyer (1959) method (Spivak, 2015). Briefly, sediments were extracted using a methanol: chloroform: phosphate buffer saline mixture (2: 1: 0.8, v: v: v) with a microwave-accelerated reaction system that heated samples to 80°C for 10 min with constant stirring. Samples were then partitioned and the organic phase removed. The total lipid extract was concentrated under nitrogen gas and elemental sulfur was removed by filtration through acid-rinsed copper. Extracts were resuspended in hexane and sequentially separated into four fractions by solid phase extraction on Discovery DSC-NH_2 stationary phase (1 g): F1 5 mL hexane; F2 8 mL of 4:1 hexane: methylene chloride; F3 10 mL of 9: 1 methylene chloride: acetone; F4 15 mL of 2% formic acid in methylene chloride (Sessions, 2006). The F4 fraction was methylated with acidic methanol (95:5, methanol: HCl) and heated overnight at 70°C to form fatty acid methyl esters. The F1 (hydrocarbons) and F4 (FAMEs) were analyzed with an Agilent 7890 gas chromatograph with the effluent split ~70: 30 between a 5975C mass spectrometer and a flame ionization detector. Compounds were separated on an Agilent DB-5 column (60 m, 0.25 mm inner diameter, 0.25 μm film). Hydrocarbon and FAMEs concentrations were quantified using a methyl heneicosanoate internal standard. Percent composition was calculated by normalizing to the total concentration.

2.5. Radiometric Dating and Accretion Rates

Soil accretion rates were constrained by developing geochronology models based on measurements of ^{7}Be, ^{137}Cs, ^{210}Pb, and ^{226}Ra on a planar-type gamma counter (Canberra, Inc. USA; Gonneea et al., 2019).

Activities of ^{226}Ra and ^{210}Pb and were then processed with the *rPlum* (0.2.2) package for R, in order to obtain Bayesian-based accretion rate estimates and 95% confidence intervals (Aquino-López et al., 2018). The model was run using measured ^{226}Ra activities as individual estimates of supported ^{210}Pb within each soil horizon. Pond accretion rates could not be obtained due to violation of steady-state assumptions (Luk et al., 2021). Total ^{210}Pb inventories within the marsh and ponds were used to estimate rates of soil erosion as described in the next section (Walling & Quine, 1994).

2.6. Pond Erosion Estimates

Erosional losses were constrained (a) by estimating wind-driven resuspension and export, and (b) from differences in total ^{210}Pb inventories between the marsh and ponds. Wave driven erosion in the ponds was estimated with a simplified model. We calculated significant wave height and peak period as a function of wind speed, fetch, and water depth using semi-empirical equations (Young & Verhagan, 1996). We then calculated the bed shear stresses using the linear wave theory (Wiberg & Sherwood, 2008) and the Swart (1974) formula for the friction factor, with an equivalent bed roughness of 0.3 mm. Wind speed estimates were based on median wind speeds (4.04 m s^{-1}) recorded by a meteorological tower in PIE-LTER located near one of ponds that has been in operation since 2013 (42.7345, −70.8382; Giblin, 2021).

We constrained wind-driven erosion based on fetch and water depth in two scenarios: one for tidally isolated ponds (i.e., the marsh platform is not inundated) and a second for when high tides inundate the marsh platform (Figure 2c). For waves generated within the ponds, we selected fetches equal to pond diameters (30–100 m) and depths calculated with respect to the surrounding marsh (i.e., assuming the pond is completely filled with water). We then considered the scenario when the marsh is inundated and selected a larger fetch (i.e., the marsh platform, 1–3 km), but a shallower depth (equal to the depth on top of the platform). In the latter case, we used the depth on top of the marsh platform to calculate the wave height, but we used the depth inside the ponds to calculate the bed shear stresses in the ponds. For both scenarios we identified the pond depths (with respect to the marsh platform) for which the bed shear stress is equal to the critical value, which was assumed equal to range from 0.1 to 0.2 Pa based on intertidal mudflats (Mitchener & Torfs, 1996). In practice, we used these two scenarios to estimate the maximum depths at which wind-driven erosion and soil export no longer take place due to bed shear stresses falling below the critical value.

We then estimated the frequency that erosion and export events co-occur by combining wind and tidal height data. From the PIE-LTER meteorological tower data, we selected representative years capturing the minimum and maximum wind speeds between 2013 and 2019 and identified periods when windspeeds were greater than 4 m s^{-1}. Within those periods we evaluated whether tidal waters were high enough to overtop the marsh platform and connect with the ponds (Spivak et al., 2017). From this combined data set we calculated frequency that high wind and water events co-occur within a year and could lead to export.

We further constrained erosional losses by calculating ^{210}Pb inventories in the marshes and ponds. We assumed that higher average total inventories of marsh cores (M1, M2) reflected a depositional environment while lower total inventories of the pond cores were due to physical removal and/or nondeposition of soil material (Walling & Quine, 1994).

2.7. Data Analysis

To evaluate how soil properties and composition change with depth in ponds and compare across the pond and marsh sites (near M1, far M2), we pooled soil horizons based on elevation relative to the marsh upper horizons (1.2–1.5 m, NAVD88) that reflect (A) marsh surface soils and emergent grass rooting zone (0–30 cm), (B) pond upper soils (0–10 cm) and marsh soils (30–40 cm) at corresponding elevations, and (C) intermediate (10–30 cm pond; 40–60 cm marsh) and (D) deeper (30–50 cm pond; 60–80 cm marsh) horizons (Figure 2b). Kolmogorov-Smirnov tests were used to evaluate normality and data were log-transformed as needed in MATLAB. Post-hoc contrasts from linear mixed models were used to test down-core changes in the marsh (M1 and M2) and pond zones as well as to assess differences between zones across these environments. Contrast coefficients and *p*-values describe the magnitude and directional difference in soil composition between environments or downcore zones and whether differences are significant. Using this approach, we further assessed across site variability by testing differences in whole-core (A–D) marsh soils (M1 and M2) across the three

Table 1
(a) Downcore and (b) Between-Environment Contrast Analyses for Soil Properties at the Pond and Near (M1) and Far (M2) Marsh Sites. Response Variables Include Soil Bulk Density, Total Nitrogen Content, Total Organic Carbon Content, C:N Ratios (Molar), and Total Organic Carbon Density

	Contrast	Bulk density $\log_{10}$ (g cm^{-3})	Total nitrogen $\log_{10}$ (%)	Total organic carbon $\log_{10}$ (%)	C:N	Total organic carbon (kg m^{-3})
a.						
POND	B–C	**−0.15**	**0.17**	0.13	−0.02	2.04
	C–D	0.09	−0.04	−0.02	0.33	2.61
	B–D	−0.06	**0.13**	−0.11	0.31	4.64
M1	B–C	−0.09	0.08	0.05	0.16	0.76
	C–D	0.01	0.02	−0.06	0.15	−1.85
	B–D	−0.08	0.10	−0.01	0.31	−1.08
M2	B–C	**−0.14**	**0.14**	0.11	**2.35**	3.98
	C–D	0.06	−0.02	0.00	0.30	2.40
	B–D	−0.08	**0.11**	0.11	**2.64**	**6.38**
b.						
A	M1–M2	−0.03	0.06	0.03	**−1.30**	−0.45
B	M1–M2	−0.02	0.03	−0.01	−1.89	−1.93
	M1–POND	0.12	**−0.12**	−0.09	1.20	1.88
	M2–POND	**0.14**	**−0.16**	−0.08	**3.09**	3.81
C	M1–M2	−0.07	**0.09**	**0.11**	0.62	2.82
	M1–POND	0.06	−0.04	0.01	1.34	4.68
	M2–POND	**0.13**	**−0.13**	−0.10	0.72	1.86
D	M1–M2	−0.02	0.05	0.07	1.07	3.37
	M1–POND	**0.14**	−0.09	−0.05	1.83	5.44
	M2–POND	**0.16**	**−0.14**	**−0.12**	0.76	2.07

Note. Contrast coefficients are presented for depth zones as described in Section 2.7 and Figure 1b. Bolded values are significant at $p < 0.05$. For example, the downcore contrast coefficient for Pond "B–C" for bulk density demonstrates that the significant difference between (B) surface and (C) intermediate pond soil properties is −0.15 $\log_{10}$ (g cm^{-3}). Between-environment contrast coefficient of B "M1–M2" represents the insignificant difference between the M1 and M2 soil properties at depth zone B.

study sites. Linear mixed models and post-hoc contrasts were conducted in R (1.3.1093) using the *lm* (4.0.0) and *lsmeans* (2.30.0) packages (R Core Team, 2022).

Because we could not develop accretion models for the ponds, statistical comparisons of marsh soil accretion rates were treated differently. To test differences in marsh accretion rates that corresponded with time-since-pond formation and distance from pond, we conducted post-hoc contrasts of mixed linear models to evaluate differences between horizons deposited before and after pond formation (Ponds 1 and 2: 1978, Pond 3: 1963; approximated by aerial photographs, Spivak et al., 2017) and marsh core location.

3. Results

3.1. Bulk Soil Properties

Downcore trends in soil bulk density and elemental content were generally similar across the ponds and marsh environments. Bulk density generally increased while %TN decreased with depth in both marshes and ponds (Table 1a, Figures 3a and 3b). Soil TOC content (%) and density (kg m^{-3}) were similar in emergent and submerged environments and tended to decrease with depth, though this was not significant (Figures 3c and 3e, Table 1a,b). Carbon-to-nitrogen (C:N) ratios were highest in the top 30 cm of marsh soils (depth zone A) but, below this, were similar in the marshes and ponds and showed little change with increasing depth (Table 1a,b, Figure 3d). Ponds generally had lower bulk densities than the marsh and higher %TN values, particularly in the upper B depth zone (M1 and M2; Figures 2 and 3; Table 1b). Soil properties and elemental content likely reflect a combination of processes, including water infiltration in pond surface horizons that results in lower bulk density, and long-term decomposition that contributes to carbon loss and compaction of deeper soils.

Similar soil properties in the top 30 cm (depth zone A) of the near and far marsh sites suggest that they are unaffected by ponding (Figure 3, Table 1b). Only C:N differed with distance from the ponds, with higher ratios in the far marsh (M2) that reflect slightly lower %TN. In contrast, there were stronger differences between soil properties in the top 30 cm (A depth zone) and deeper depth zones (B-D; Table S1 in Supporting Information S1). Lower bulk densities and higher %TOC and %TN in the top 30 cm are consistent with the active rooting zone.

3.2. SOC Sources and Reactivity

We assessed SOC sources and reactivity in the ponds and far marsh soils (M2) with a combination of stable isotopes, lipid biomarkers, and thermal indices to evaluate potential shifts in organic matter inputs that could be indicative of erosion and decomposition (Figures 4 and 5, Tables 2–4). Soil δ^{13}C and δ^{15}N values ranged from −17 to −11‰ and 0.74–7.17‰, respectively, reflecting salt marsh-derived organic matter (Figure 4, Table 2; Spivak & Ossolinski, 2016). Soil δ^{13}C values were similar across depths and between marsh and pond environments, with the exception of horizon B where pond values were comparatively depleted (Figures 4a, Table 2). In contrast, δ^{15}N values were lower in ponds compared to the marsh (Figures 4b, Table 2c). The reactivity proxy, t50, increased with depth in marsh soils indicating a shift toward greater thermal stability (Figures 4c, Table 2). Interestingly, t50 values were highest in pond surfaces (depth zone B, Table 2c) but decreased and converged with marsh values below this (depth zones C, D, Table 2c). Stable isotopes and t50 reflect the entire SOC pool so in order to gain greater insight into sources and transformations we used fatty acid and hydrocarbon lipid biomarkers.

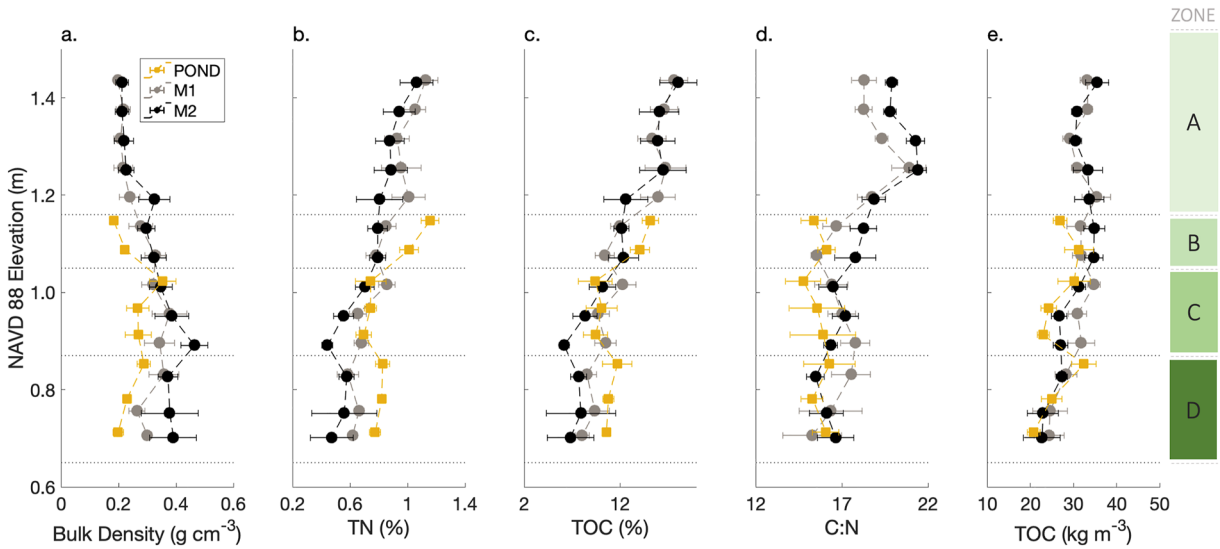

Figure 3. Pond and marsh (near: M1; far: M2) soil (a) bulk density, (b) total nitrogen (TN) content (TN %), (c, e) total organic carbon (TOC) content and density (TOC % and kg m^{-3}), and (d) C:N ratios (molar) by elevation and depth horizon. Data represent mean and SE of 6 cm increments. See methods and Figure 2b for descriptions of the depth zones A-D and Table 1 for contrast analyses.

The total FA were primarily comprised of long-chain (LCFA) and short chain (SCFA) saturated compounds with smaller contributions of monounsaturated (MUFA), branched (BrFA), polyunsaturated (PUFA), and linoleic and linolenic ($C_{18:2}$ + $C_{18:3}$) compounds (Figure 5, Figure S1 in Supporting Information S1; Table 3). Levels of %SCFA, %MUFA, and %PUFA were higher in pond surface soils and decreased with depth (Figures 5a, 5b, and 5e; Tables 3–4). In contrast %SCFA and %PUFA were constant with depth in the marsh, while %MUFA was higher in surface soils. Bacterial contributions, represented by BrFA, were similar in pond horizons B and C, but decreased with depth in the marsh (Figures 5d, Table 4). Vascular plant contributions, represented by %LCFA, were lower in pond surface horizons and increased with depth (Figures 5c, Table 4). In contrast, two

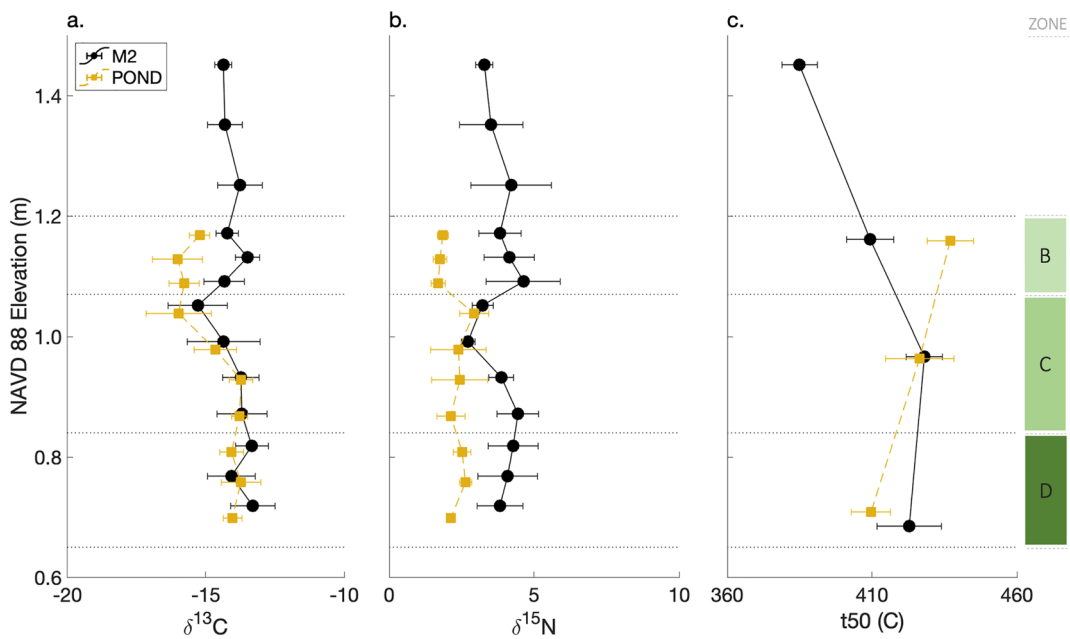

Figure 4. (a and b) Stable isotope composition (δ^{13}C, δ^{15}N; ‰) and the (c) thermal reactivity proxy t50 of pond and marsh (M2, far) soils. The t50 represents temperatures at which 50% of soil organic carbon is pyrolyzed. Data are mean and SE. Statistical results in Table 2.

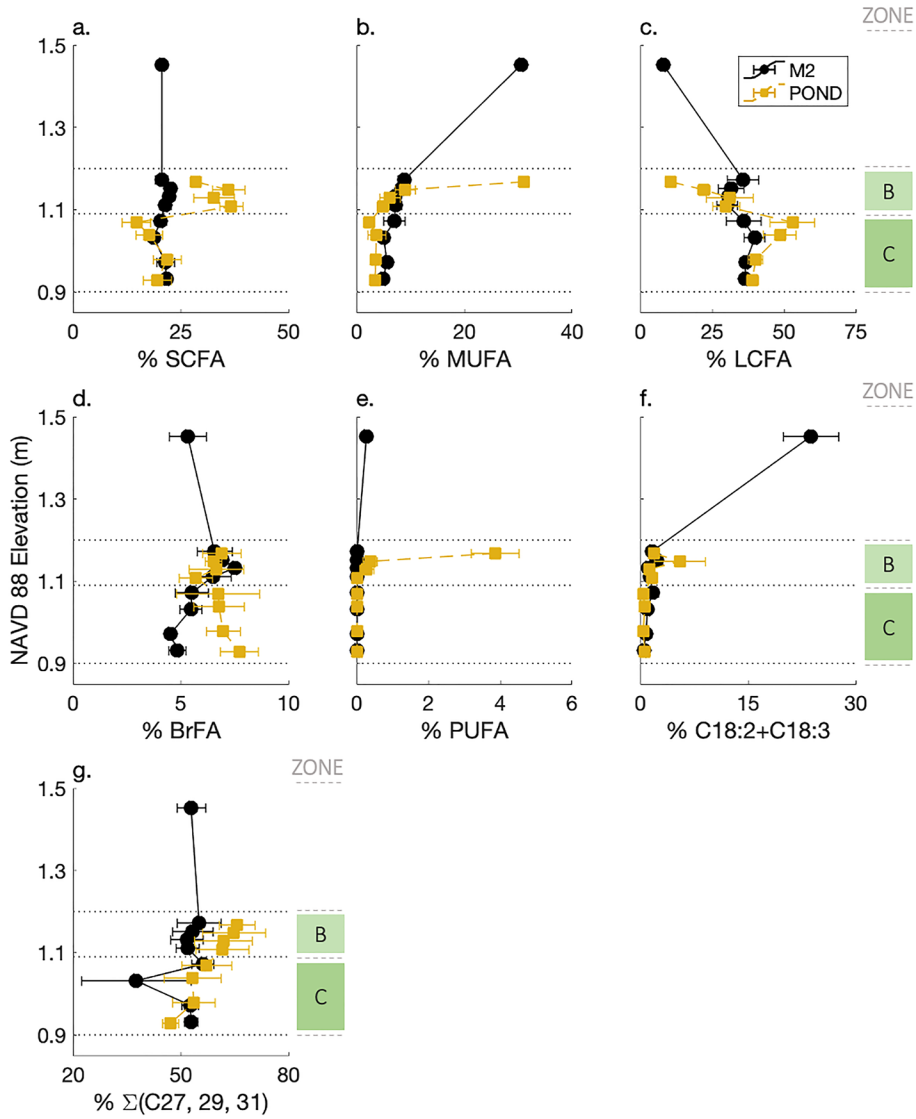

Figure 5. Relative abundances of (a) short chain FAs (SCFA), (b) monounsaturated FAs (MUFA), (c) long chain FAs (LCFA), (d) branched FAs (BrFA), (e) polyunsaturated FAs (PUFA), (f) $C_{18:2} + C_{18:3}$, and (g) odd-chain n-alkanes in ponds and M2 marsh sites. Data are the mean and SE. See Section 2.7 for a description of soil zones, Table 3 for source information, and Table 4 for statistical results.

compounds produced by *S. alterniflora* and *Ruppia maritima*, linoleic and linolenic FAs, were higher in surface horizons, particularly in the marsh, but declined with depth (Figures 5f, Table 4). In general, marsh soil profiles of the percent contributions of different FA groups were less variable than the ponds, with some evidence of decomposition as slight increases in %LCFA and decreasing microbial contributions (%MUFA, %SCFA, %PUFA) from surface to depth (Figure S1 in Supporting Information S1). Ponds, in contrast, had higher contributions of algal lipids in surface horizons, reflecting colonization by benthic microalgae (Spivak et al., 2018), and greater evidence of decomposition as sharper shifts in %SCFA, %MUFA, %PUFA, and %LCFA with depth.

We used hydrocarbons to evaluate contributions from vascular plant detritus. In the marsh, contributions of long-chain n-alkanes were relatively constant with depth (Figure 5g; Tables 3 and 4). In contrast, levels were higher in pond surfaces and decreased by ~10% with depth. Greater percent contributions in pond surface horizons compared to the marsh suggest either increased deposition of plant detritus or a changing decomposition environment that facilitates an accumulation of these compounds. In combination, our data indicate that pond surface soil horizons were distinct from the surrounding marsh, with greater contributions from algae and

Table 2
Contrast Coefficients of Soil Stable Isotope Composition ($\delta^{13}C$, $\delta^{15}N$; ‰) and Thermal Reactivity (t50) Between Depth Horizons Within (a and b) and Across (c) the Pond and Far Marsh (M2) Environment

	Contrast	$\delta^{13}C$	$\delta^{15}N$	t50
a.				
POND	B–C	−1.14	−0.71	10.50
	C–D	−0.60	0.05	16.93
	B–D	**−1.74**	−0.66	27.43
b.				
M2	B–C	0.25	0.64	−18.80
	C–D	−0.69	−0.50	5.22
	B–D	−0.44	0.13	−13.58
c.				
M2–POND	B	**1.66**	**2.44**	**−27.72**
	C	0.27	**1.09**	1.58
	D	0.37	**1.64**	13.28

Note. Significant values ($p < 0.05$) are bolded.

microbes and shifts in reactivity proxies that are consistent with microbial processing.

3.3. Soil Radioisotopes

We assessed whether marsh vertical accretion rates differed with distance from the ponds or changed after the approximate year of pond formation (data available in USGS ScienceBase, Luk et al., 2020). Mean vertical accretion rates at sites closer (M1) and farther (M2) from the ponds ranged from 4.78 to 5.12 mm yr^{-1} (Figure 6), exceeding local sea-level rise (SLR) rates (2.87 ± 0.15 mm yr^{-1}; NOAA station #8443970). In the farther marsh site (M2), accretion rates accelerated after 1963–1978, which roughly coincides with the appearance of the ponds in aerial images (Table 5). However, in the early 2000s (~1.35 m NAVD 88), accretion rates at both the near (M1) and far (M2) marsh locations converged to an average of 5.10 mm yr^{-1}. These accretion rates indicate that the marshes gained 6.8–9.7 cm in elevation since the ponds formed, which accounts for 22%–33% of pond depths.

We also used ^{210}Pb to assess if net accretion occurred in the ponds after formation. Based on pond elevations, it is apparent that if any accretion occurred, it would be at rates suppressed compared to the platform. In addition, given the proximity of the pond and platform cores, similar ^{210}Pb atmospheric deposition rates are expected. As a result, if sediment accretion occurred in the ponds, we would expect higher ^{210}Pb activities at lower accretion rates, however the opposite is observed with ^{210}Pb activities in pond surface sediments significantly depressed compared to marsh surface activities. In fact, the ^{210}Pb activities are comparable at similar elevations across pond and platform cores. As a result, soil radioisotope inventory differences between pond and platform environments informed diffusion-migration erosion models. Mean ^{210}Pb inventories in the marsh cores were 5,576 Bq m^{-2}, and ranged from 4,137 to 7,835 Bq m^{-2}. Inventories in the pond soils were much lower, ranging from 517 to 2,915 Bq m^{-2}.

Table 3
Lipid Classes and Sub-Classes Used to Assess Organic Matter Sources in Marsh and Pond Soils

Lipid class	Compounds	Sources	References
Fatty acids			
Short chain fatty acids (SCFA)	$\Sigma(C_{12:0}, C_{14:0}, C_{16:0}, C_{18:0})$	Microbes, algae, and some vascular plants	Jeffries (1972), Canuel et al. (1997), Sessions (2006)
Monounsaturated fatty acids (MUFA)	$\Sigma(C_{14:1}, C_{16:1}, C_{17:1}, C_{18:1}, C_{19:1}, C_{20:1}, C_{22:1}, C_{24:1})$	Bacteria, microalgae, macroalgae. Trace in *S. alterniflora*	Volkman et al. (1980, 1989), Kaneda (1991), Viso and Marty (1993), Fleurence et al. (1994), Canuel et al. (1997), Sessions, 2006
Polyunsaturated fatty acids (PUFA)	$\Sigma(C_{20:4}, C_{20:5}, C_{22:5}, C_{22:6})$	Microalgae	Volkman et al. (1989)
Branched fatty acids (BrFA)	iso- and anteiso- Σ (C_{13}, C_{15}, C_{17}, C_{19})	Bacteria	Kaneda (1991)
Long chain fatty acids (LCFA)	$\Sigma(C_{24:0}, C_{26:0}, C_{28:0}, C_{30:0})$	Vascular plants	Bianchi and Canuel (2011)
Linoleic and linolenic fatty acids	$C_{18:2} + C_{18:3}$	*S. alterniflora*, *R. maritima*, microalgae	Jeffries (1972), Volkman et al. (1989), Canuel et al. (1997)
Hydrocarbons			
Long-chain n-alkanes	$\Sigma(C_{27}, C_{29}, C_{31})$	*S. alterniflora* and to a lesser extent *R. maritima*	Canuel et al. (1997), Sessions (2006)

Note. Fatty acids and hydrocarbons represent fresher and more detrital material, respectively.

Table 4
Contrast Coefficients of Short Chain FAs (SCFA), Monounsaturated FAs (MUFA), Long Chain FAs (LCFA), Branched FAs (BrFA), Polyunsaturated FAs (PUFA), $C_{18:2}$ + $C_{18:3}$, and Odd-Chain n-Alkanes ($\Sigma(C_{27},C_{29},C_{31})$) (a) Between Depth Horizons Within and (b) Across the Ponds and the Far Marsh (M2) Site

	Contrast	%SCFA	%MUFA	%LCFA	%BrFA	%PUFA	%C18:2 + C18:3	%∑(C27, 29,31)
a.								
B–C	POND	**0.50**	**0.50**	**−21.77**	−0.61	0.02	**0.34**	**10.30**
	M2	0.15	0.15	−5.17	**1.79**	0.00	0.20	3.20
b.								
M2–POND	B	**−11.78**	−0.07	**8.66**	0.44	−0.02	−0.16	**−10.09**
	C	2.14	**0.28**	**−7.94**	**−1.97**	0.00	−0.02	−3.01

Note. Significant values ($p < 0.05$) are bolded. Because zone A only includes the M2 surface and does not have a pond complement it was excluded from statistical analyses. To meet assumptions of normality, %PUFA, %C18:2 + C18:3, and %MUFA were log-transformed prior to contrast analyses.

3.4. Estimating Pond Erosion

Pond erosion rates were constrained using radioisotope-based and physical models and by assuming negligible contributions of root collapse to deepening. A diffusion-migration model (Walling & Quine, 1994) based on total ^{210}Pb inventories of the marsh and pond soils, yielded erosion rates of 4–10 cm yr^{-1} (7.7–11.4 kg soil m^{-2} yr^{-1}). We also developed simple wind-driven erosion models, based on the two fetch and water depth scenarios (see Section 2.6 and Figure 2c), that provided estimates of critical pond depths at which erosion and resuspension were possible. When fetch is limited to pond diameters, critical depths for resuspension are 1.8–5.4 cm, but when fetch is 1–3 km across the flooded marsh, critical depths span a wider range of 0.1–12 cm. By combining pond soil bulk densities (Figure 3a), radioisotope-based erosion rates, and pond ages approximated from aerial images (Spivak et al., 2017) with a 12 cm critical depth from the wave model, we estimate maximum erosive losses of 14.4–26.4 kg soil m^{-2} (2.5–3.0 kg C m^{-2}) from the three ponds. These figures represent maximum potential losses from pond formation to 2014, rather than progressive expansion over time, but would likely occur in the first few (2–3) years. Soil export from the ponds would only occur during simultaneous high wind and high-water events. Roughly 33% of high tides per year are sufficient to hydrologically connect ponds to tidal channels, based on observations by Spivak et al. (2017). Windows for erosive losses narrow to ∼17% of high tides, based on co-occurrence of wind and tide events during low (2014) and high (2013) wind years. Soil export during coinciding events would be uneven and possibly concentrated to a few strong storms. Overall, our models demonstrate that sediment can be resuspended efficiently in very shallow water depths even though the marsh is only submerged a small fraction of the time.

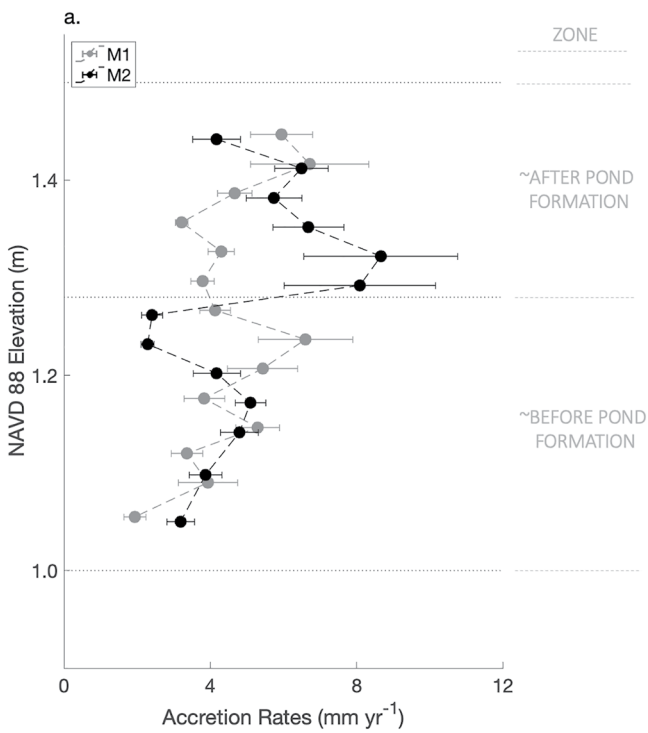

Figure 6. Accretion rates in marshes closer (M1) and farther (M2) from the ponds. Mean rates are based on 3 cm increments and error bars represent SE. Zones after and before pond formation correspond to horizons above and below the year 1978 (Pond 1 and Pond 2) and 1963 (Pond 3), respectively, which is approximately when the ponds formed (∼1.3 m NAVD88). See Table 5 for contrast analyses.

4. Discussion

4.1. Ponding Effects Are Spatially Constrained

Pond expansion occurs at the expense of the vegetated marsh: grasses dieback, mudflats form, and soils are lost, forming depressions that widen and deepen over time (Figure 1; DeLaune et al., 1994; Mariotti & Fagherazzi, 2013; Wilson et al., 2014). Because of this lateral expansion, we expected that ponds may influence the physical structure and composition of surrounding marsh soils. Instead, we found that the bulk density and elemental composition of marsh soils were similar at differing distances from the ponds (∼10 vs. ∼20 m; Figure 3, Table 1b). This indicates that ponding effects on the marsh are largely constrained to within a 10 m perimeter or smaller and do not

Table 5
Contrast Analyses of Marsh Accretion Rates (a) Between and (b) Within the Near (M1) and Far (M2) Marsh Sites After and Before Pond Formation (1963–1978)

a.		b.	
Accretion rate (M1—M2)		Accretion rate (before—after)	
Contrast	Coefficient	Contrast	Coefficient
After pond	**−0.08**	M1	−0.01
Before pond	**0.09**	M2	**−0.02**

Note. Coefficients $p < 0.05$ are bolded.

reduce the integrity of this system more widely. Ponds are however enlarging, and thus converting the surrounding "undisturbed" marsh into an open water environment but higher spatial resolution sampling is needed to assess their zone of influence.

Below the marsh grass rooting zone, soil properties were fairly constant with slight increasing trends in bulk density and decreasing C:N ratios that likely reflect a combination of decomposition, soil compaction, and immobilization of nitrogen into microbial biomass and necromass (zone A, 0–30 cm, 1.18–1.48 m NAVD 88, Figure 3, Table 1a; Goñi and Thomas, 2000; Luk et al., 2021; Wang et al., 2003). Little variation in bulk density and organic matter content might suggest that the processes building soils are similar across the marsh, however, changing vertical accretion rates point to a more dynamic system (Figure 6, Table 5). Average accretion rates at the M2 sites were variable, slowing and then accelerating during the years bracketing 1963–1978. It is unlikely that these changes are related to pond formation and expansion since they are not apparent at the closer M1 sites. It is more likely that changing vertical accretion rates are associated with temporally and spatially stochastic processes. Soils eroded from tidal channels and mosquito ditches can be redeposited on the marsh platform but the extent and frequency of redistribution is an open question (Hopkinson et al., 2018; Luk et al., 2021). Strong winter storms can deposit sediment-laden ice from bays and tidal creeks onto the marsh platform (Argow et al., 2011; Baranes et al., 2022; Chmura et al., 2001; Reed, 1989; Schuerch et al., 2012). An example is a 2018 extratropical cyclone that delivered sediment equivalent to years of natural accumulation (FitzGerald et al., 2020). The sudden jump in accretion rates at the M2 sites happened in the two cores closest to a mosquito ditch (12 m, site 1) and tidal channel (22 m, site 3) and is consistent with episodic deposition. Another option is that rapid accretion followed infilling of relict ponds (Wilson et al., 2014) but this is unlikely as these features are not apparent in historical aerial photographs. Spatial and temporal heterogeneity in vertical accretion rates may also reflect factors such as changes in marsh grass species, abundance, and productivity (Bricker-Urso et al., 1989; Friedrichs & Perry, 2001; Turner et al., 2002). Although we cannot link variability in accretion to ponding, our results demonstrate that rates have increased over the past ∼100 years from 2.89 to 4.59 mm yr^{-1}, which is comparable to relative SLR rates of 2.89 ± 0.15 mm yr^{-1} (NOAA station #8443970), and highlight that assessment of spatial and temporal heterogeneity is limited to the density and location of cores across the gradient of relevant drivers, as well as the temporal precision of the age model developed.

4.2. Pond Soils Reflect Changing Organic Matter Inputs and Decomposition

Pond surface areas and depths vary widely within and across marsh ecosystems (Adamowicz & Roman, 2005; Millette et al., 2010). Current models invoke varying combinations of physical and biogeochemical processes to describe pond formation and expansion over time (Himmelstein et al., 2021; Mariotti, 2016; Mariotti et al., 2020). Yet, it remains unclear whether submergence effects on biogeochemical transformations extend below surface sediments and propagate into the underlying peat. Better constraining the processes contributing to deepening has implications for the controls on pond depths and our understanding of peat vulnerability to decomposition when environmental conditions change.

Compositional differences between pond surface sediments and the surrounding marsh reflect both new inputs from the communities that established following submergence and microbial reworking of older organic matter. More depleted $\delta^{13}C$ and $\delta^{15}N$ values, higher nitrogen content, and greater %SCFA, %PUFA, and %MUFA contributions in upper pond horizons (0–10 cm, 1.1–1.2 m NAVD 88), compared to the marsh, likely reflect newer inputs from benthic microalgae and soil microbes (Figures 3–5; Tables 1–4; Spivak & Ossolinski, 2016; Spivak et al., 2018). This is consistent with previous findings that benthic microalgae and, to a lesser extent, suspended particulate organic matter, are the main carbon sources in pond surface soils (0–2 cm), based on phospholipid-linked fatty acids (PLFAs) and isotope mixing models (Spivak et al., 2018). The submerged grass, *R. maritima* that established following permanent inundation, also produces $C_{16:0}$ at fairly high levels and likely contributed to the peak in %SCFAs in the upper pond horizons, as this corresponds with its rooting zone (Henninger et al., 2009; Jeffries, 1972). New inputs likely dilute older contributions as %LCFA were relatively lower in the upper pond horizons compared to the marsh (0–10 cm; 1.1–1.2 m NAVD 88) but increased with

depth (Figure 5c; Table 4). Although pond surface sediments accumulate organic matter from recently established submerged communities, substantially lower radioisotope inventories and lower elevations compared to the marsh indicate that they are not net depositional environments. Any minor deposition that may occur during high energy events is not reflected in sedimentary record and would thus be transitory in nature and not add to net accretion.

Disturbances that cause marsh peat collapse can decrease soil bulk density and alter the decomposition environment (Chambers et al., 2019; Day et al., 2011; Wilson et al., 2018). Consistent with this, ponds had lower bulk densities compared to the marsh and shifts in organic matter composition and reactivity that reflect microbial processing (Figures 3–5). Levels of the n-alkanes C_{27}, C_{29}, and C_{31}, representing more detrital organic matter sources, compared to FA, were relatively higher in pond surface sediments than the marsh (i.e., 1.1–1.2 m NAVD 88, Figures 5g, Table 4b). Both *S. alterniflora* and *R. maritima* produce these compounds, but the former has higher levels, particularly of C_{29} (Tanner et al., 2010). Higher t50 values in the pond surfaces, compared to the marsh and deeper soil horizons, are consistent with an accumulation of more stable, detrital compounds (Figures 4c, Table 2; Lehmann et al., 2020; Luk et al., 2021; Williams & Rosenheim, 2015). Because thermochemical properties reflect the bulk SOC pool, further molecular characterization (e.g., nuclear magnetic resonance) would be needed to assess how selective preservation and microbial reworking contribute to the shift in stability (Sanderman & Grandy, 2019; Williams & Plante, 2018; Yang et al., 2006). Potential insight from bacterial FA, which comprised similar fractions of organic matter in the upper pond horizons and the marsh (% BrFA; Figure 5, Table 4), is limited as other, more sensitive biomarkers (e.g., PLFAs) or molecular approaches (e.g., ribonucleic acids) are better proxies of microbial activity and community composition (Bulseco et al., 2020). Regardless of the process driving the shift, greater thermal stability is associated with longer SOC turnover times, which may slow continued deepening and peat loss (Luk et al., 2021).

Below the upper pond horizons and rooting depth of *R. maritima*, (0–10 cm; 1.1–1.2 m NAVD 88) soil properties and composition were similar to the surrounding marsh, underscoring that ponds overlie salt marsh peat (Figures 3–5). For instance, soil bulk densities, elemental content, lipid biomarker profiles, and thermal properties were similar between the ponds and the marsh below ∼1.1 m NAVD 88 (Zone C–D; Figures 3–5, Tables 1, 2, and 4). Soil $\delta^{13}C$ values converged to $-14.3 \pm 1.2‰$ (Figure 4a; Table 2), indicating that buried carbon mainly derives from marsh grasses (Benner et al., 1987; Spivak & Ossolinski, 2016). The exceptions to this pattern were $\delta^{15}N$ values and bacterial FA which were lower and higher, respectively, in deeper pond horizons compared to the marsh (Figures 4b and 5d; Tables 2 and 4). Coincidentally, porewater profiles of microbial respiratory products (i.e., dissolved inorganic carbon [DIC], ammonium) and electron acceptors (i.e., sulfate) in pond sediments demonstrate that production and consumption, respectively, occur to at least 20 cm depth (Spivak et al., 2018). Further, $\delta^{13}C$ values of branched PLFAs and porewater DIC suggest that soil microbes are partially reliant on buried peat (Spivak et al., 2018). While ponding effects on sediment physical structure and organic matter composition are largely limited to upper horizons (i.e., 0–10 cm, 1.1–1.2 m NAVD88; Figures 3–5) changes in the belowground environment that influence bacterial communities may extend deeper.

Overlaying proxies of organic matter sources and reactivity allowed us to differentiate new inputs (Figures 5a and 5e) from transformations consistent with microbial reworking (Figures 4c and 5g). Accumulation of senesced biomass from submerged primary producers in pond sediments is likely limited by substantial heterotrophic microbial demand (i.e., high respiration rates) and a favorable decomposition environment (Spivak et al., 2017, 2018, 2020). This is consistent with laboratory and landscape-scale experiments in which simulated disturbances increase the bioavailability of buried marsh organic matter to microbes (Bowen et al., 2009; Bulseco et al., 2019, 2020; Spivak et al., 2018). Over time this has resulted in a shift toward an accumulation of more stable SOC in pond surfaces, whether by way of selective preservation or microbial alteration (Figures 4c and 5g). If thermal properties reflect bioavailability, then shifts toward more stable SOC may slow rates of pond deepening via decomposition. While contrasting SOC composition between pond surfaces and the nearby marsh points to decomposition, we cannot ascertain the relative importance of this process as a driver of organic matter loss compared to erosion with this set of biomarkers and proxies.

4.3. The Fate of Carbon During Pond Expansion

Ponds can reduce salt marsh soil carbon storage by preventing new burial and facilitating loss of long-buried organic matter (Wilson et al., 2009, 2010). The present-day water-filled volumes of the ponds represent soil carbon stocks that are missing from the wider ecosystem. The size of the missing carbon stocks is estimated from

Table 6
Carbon Stocks Missing From Ponds Can Be Attributed to Avoided Accretion, Erosion, and Decomposition

	Site	Pond age	Avoided accumulation (%)	Erosion loss (%)	Decomposition loss (%)	Decomposition rate (g C m^{-2} y^{-1})
a						
	1	38	32	35	33	62
	2	38	37	38	25	53
	3	51	42	36	22	33
b						
	1	38	32	0	68	129
	2	38	37	0	63	133
	3	51	42	0	58	86

Note. Estimated contribution of each process when erosion losses are greatest (a) or minimal (b).

pond volumes (Spivak et al., 2017) and by assuming that the soil carbon density would have been equivalent to the marsh (33.1 kg C m^{-3}; Figure 3). Three processes that could account for the missing carbon are avoided (or prevented) accretion and removal via erosion and decomposition. Since the ponds formed, the marshes gained 6.8–9.7 cm in elevation and accumulated 59.5–79.3 g C m^{-2} yr^{-1}; this represents avoided accretion and accounts for 32%–42% of the missing carbon stock.

Erosion effects on pond deepening would have been limited to the first few years when the systems were shallowest. We estimate that winds could have resuspended and facilitated export of up to 14.4–26.4 kg m^{-2} of soil from the ponds within the first 2–3 years of forming, based on the longer fetch scenario and deepest critical depth of 12 cm (Figure 2c). Maximum erosion losses could reach 2.5–3.0 kg C m^{-2}, constituting up to 35%–38% of the missing pond carbon (Table 6a). This an upper bound because we assumed that peat collapse did not contribute to deepening and that all resuspended soil is exported. The likelihood of export, however, would be limited to coinciding high wind events and tides that hydrologically connect ponds to channels, and could be limited to a few strong storms. The frequency at which soils are resuspended and exported likely slows over time, as the ponds deepen and the fraction of surface water exchanged during high tides decreases. For instance, small changes in water temperatures, dissolved oxygen concentrations, levels of suspended particulate organic matter over periods of tidal connection and isolation suggest that the ponds are not strongly flushed when the marsh floods (Spivak et al., 2017). However, stochastic events, such as strong storms that arrive during high tides, have the potential to move substantial amounts of sediment (FitzGerald et al., 2020). In some systems, the dominant wind direction and storms that follow predictable tracks can affect the shapes of expanding ponds, with a net effect of longer fetches and greater potential for erosion (Ortiz et al., 2017; Stevenson et al., 1985). Wind-driven resuspension may also indirectly contribute to carbon loss, by moving particles from anoxic sediments into oxic surface waters where decomposition may be more likely (Abril et al., 1999; Boynton et al., 1981). Further constraining potential erosive losses requires high resolution monitoring of pond turbidity, water levels, and temporal changes in spatial attributes, as well as capturing storm events.

After accounting for accretion and potential erosion, the remaining fraction of the missing carbon stock (22%–68%) is attributed to decomposition (Tables 6a and 6b). This corresponds to 32.7–132.9 g C m^{-2} yr^{-1} (see Section 3.4), which is comparable to benthic respiration (11–92 g C m^{-2}; Spivak et al., 2018) and whole-pond metabolism rates (68–172.2 g C m^2 yr^{-1}; Spivak et al., 2017, 2020). Decomposition is also consistent with the accumulation of detrital vascular plant organic matter and more thermally stable organic carbon in pond surface soils (Figures 4c and 5g; Luk et al., 2021). The respired carbon can be taken up by primary producers in the pond and recycled or lost via DIC export or CO_2 evasion to the atmosphere. Unusually enriched $\delta^{13}C$ values of pond primary producers indicate that some fraction is recycled, however, high sediment respiration rates and whole-pond net heterotrophy suggest that much of the respired carbon is lost (Spivak et al., 2017, 2018, 2020). Finally, assuming that the bulk density of buried organic matter is 85 kg m^3 (Morris et al., 2016), and that the carbon content of the organic matter is 50% by mass, a decomposition rate of 32.7–132.9 g C m^{-2} yr^{-1} corresponds to an active deepening rate of 0.8–3.1 mm yr^{-1}, which is consistent with a rate of 3 mm yr^{-1} estimated from a marsh evolution model (Mariotti et al., 2020).

The processes contributing to pond formation and deepening prevent burial and represent pathways of carbon loss or recycling within the system. We estimate that prevented burial, erosion, and decomposition account for 32%–42%, 0%–38%, 22%–68% of the carbon that is missing from the marsh due to the formation of ponds of similar ages and sizes. The contribution of prevented accretion is similar to prior estimates while that of decomposition is considerably smaller (Spivak et al., 2017, 2018). This difference likely reflects prior assumptions of lower marsh SOC content (7%; Deegan et al., 2012; Spivak et al., 2017) and extrapolation of seasonal respiration rates to longer timescales (Spivak et al., 2017, 2018, 2020), as well as our current approach of equating decomposition with the fraction of missing carbon that is not attributable to prevented accretion or erosion (Table 6). The wide estimates of missing carbon fates also reflect differences in pond sizes and ages, our approach of bracketing erosional losses with minimum and maximum values, and unknown contributions of root collapse to deepening, among other uncertainties. Refining erosion estimates further would also benefit from high resolution water level and turbidity data to constrain resuspension and export. Regardless, our current and prior findings indicate that decomposition and erosion can represent important carbon loss pathways, but with very different implications. Decomposition of long-buried organic matter returns inorganic carbon to the atmosphere or the coastal ocean. Eroded soil has the potential to be redistributed within the salt marsh system and contribute to burial and accretion elsewhere (Hopkinson et al., 2018; Luk et al., 2021). However, resuspension in oxic tidal waters may facilitate decomposition, contributing to high coastal pCO_2 levels, as little of this material is likely to survive export and burial in nearshore sediments (Canuel & Martens, 1993, 1996).

4.4. Incorporating Ponds Into Ecosystem Carbon Budgets

Although ponds are found in salt marshes worldwide (Adamowicz & Roman, 2005; Boston, 1983; Rigaud et al., 2018; Schepers et al., 2017), they are rarely included in ecosystem carbon budgets. In PIE-LTER, the 6% of area occupied by ponds in the ~40 km^2 marsh (Mariotti et al., 2020; Millette et al., 2010; Wilson et al., 2014) reduces marsh-wide soil carbon stocks to 1 m depth by ~5%. This is likely an upper bound due to redeposition of eroded material and because peat deposits are deeper than 1 m in the PIE marshes (Cavatorta et al., 2003; Luk et al., 2021; Wilson et al., 2014). Ponds therefore represent a small source of error in this system, particularly with respect to other sources of uncertainty and overall spatial heterogeneity (Holmquist et al., 2018), even though they have been expanding in recent decades due to ditch naturalization (Wilson et al., 2014).

Pond expansion may represent a larger uncertainty of soil carbon stocks of submerging marshes (Mariotti, 2016; Morris et al., 2002). For example, ponds occupy far greater fractions of marsh extent in the Blackwater River system (Maryland) and Mississippi River Delta Plain (Louisiana) (Ortiz et al., 2017; Penland, 2002; Schepers et al., 2017). This preponderance of ponds, compared to the marshes of PIE, is likely the result of a small tidal range, high rate of relative SLR, and low sediment supply (Mariotti, 2016). Given that pond expansion would take place before the marsh platform starts to drown (Mariotti, 2016), carbon might be lost faster than previously estimated from models that do not include pond dynamics (Herbert et al., 2021).

A promising approach to include the effect of pond dynamics in the marsh carbon budget is to use spatially integrative metrics that can be estimated from remote sensing, such as the Unvegetated-Vegetated marsh Ratio (UVVR) (Ganju et al., 2022). Detailed studies should investigate if the "missing" carbon due to the presence of ponds can be empirically correlated to the UVVR, and more specifically at what scale of spatial aggregation the UVVR needs to be calculated in order to best represent ponds as opposed to mudflats areas or channels.

5. Conclusions

Pond expansion threatens to contribute to salt marsh loss (Cavatorta et al., 2003; Hartig et al., 2002; Mariotti, 2016; Mariotti & Fagherazzi, 2013) and an important unknown is the fate of lost soil carbon. We demonstrate that erosion and decomposition can play key roles in pond expansion and progressive deepening. The relative importance of those processes likely changes over time, with greater erosive losses during the first years and decomposition increasingly eating away at long buried marsh peat. We estimate that erosion and decomposition account for roughly two thirds of carbon lost due to ponding in PIE but those fractions may differ in marshes with different soil types, plant species, tidal ranges, elevation within the tidal frame, and rates of relative SLR, among other processes. Shifts in environmental conditions associated with pond expansion facilitated microbial access to long-buried peat resulting in a shift toward an accumulation of detrital, vascular plant biomarkers and

more thermally stable organic matter. Though pond extent has been slowly increasing in PIE, runaway expansion is not currently a problem and there is evidence of pond draining, infilling, and recovery (Wilson et al., 2014). Importantly, pond effects on the surrounding PIE marshes are constrained to within 10 m perimeters and, at low densities, are unlikely to have destabilizing effects on the wider platform.

Conflict of Interest

The authors declare no conflicts of interest relevant to this study.

Data Availability Statement

Data are archived at BCO-DMO.org (Spivak, 2020a, 2020b, 2020c, and 2020d) and sciencebase.gov (Luk et al., 2020).

Acknowledgments
Thanks to M. Fendrock for help in collecting soil cores; M. Otter for elemental and stable isotope analyses; M. Lardie, J. Hemingway, and V. Galy for assisting with RPO analyses. This manuscript was improved by comments and suggestions from three anonymous reviewers. We are also grateful for support and assistance from PIE-LTER (NSF- OCE -1238212). Funding support was provided by NSF (NSF-OCE-1233678; NSF-DEB-2121019), Woods Hole Sea Grant (NA14OAR4170104), and NOAA (NA14NOS4190145) grants to ACS. Additional support was provided by the U.S. Geological Survey Coastal and Marine Hazards and Resources Program. Any use of trade, firm or product names is for descriptive purposes only and does not imply endorsement by the U.S. Government. The authors declare that no funds, grants, or other support were received during the preparation of this manuscript.

References

Abril, G., Etcheber, H., Le Hir, P., Bassoullet, P., Boutier, B., & Frankignoulle, M. (1999). Oxic/anoxic oscillations and organic carbon mineralization in an estuarine maximum turbidity zone (The Gironde, France). *Limnology & Oceanography*, *44*(5), 1304–1315. https://doi.org/10.4319/lo.1999.44.5.1304

Adamowicz, S. C., & Roman, C. T. (2005). New England salt marsh pools: A quantitative analysis of geomorphic and geographic features. *Wetlands*, *25*(2), 279–288. https://doi.org/10.1672/4

Aquino-López, M. A., Blaauw, M., Christen, J. A., & Sanderson, N. K. (2018). Bayesian analysis of ^{210} 210 Pb dating. *Journal of Agricultural, Biological, and Environmental Statistics*, *23*(3), 317–333. https://doi.org/10.1007/s13253-018-0328-7

Argow, B. A., Hughes, Z. J., & FitzGerald, D. M. (2011). Ice raft formation, sediment load, and theoretical potential for ice-rafted sediment influx on northern coastal wetlands. *Continental Shelf Research*, *31*(12), 1294–1305. https://doi.org/10.1016/j.csr.2011.05.004

Baranes, H. E., Woodruff, J. D., Geyer, W. R., Yellen, B. C., Richardson, J. B., & Griswold, F. (2022). Sources, mechanisms, and timescales of sediment delivery to a New England salt marsh. *Journal of Geophysical Research: Earth Surface*, *127*(3), e2021JF006478. https://doi.org/10.1029/2021JF006478

Barbier, E. B., Hacker, S. D., Kennedy, C., Koch, E. W., Stier, A. C., & Silliman, B. R. (2011). The value of estuarine and coastal ecosystem services. *Ecological Monographs*, *81*(2), 169–193. https://doi.org/10.1890/10-1510.1

Benner, R., Fogel, M. L., Sprague, E. K., & Hodson, R. E. (1987). Depletion of ^{13}C in lignin and its implications for stable carbon isotope studies. *Nature*, *329*(6141), 708–710. https://doi.org/10.1038/329708a0

Bianchi, T. S., & Canuel, E. A. (2011). *Chemical biomarkers in aquatic ecosystems*. Princeton University Press. https://doi.org/10.1515/9781400839100

Bligh, E. G., & Dyer, W. J. (1959). A rapid method of total lipid extraction and purification. *Canadian Journal of Biochemistry and Physiology*, *37*(1), 911–917. https://doi.org/10.1139/y59-099

Boston, K. G. (1983). The development of salt pans on tidal marshes, with particular reference to south-eastern Australia. *Journal of Biogeography*, *10*(1), 1–10. https://doi.org/10.2307/2844578

Bowen, J. L., Crump, B. C., Deegan, L. A., & Hobbie, J. E. (2009). Salt marsh sediment bacteria: Their distribution and response to external nutrient inputs. *The ISME Journal*, *3*(8), 924–934. https://doi.org/10.1038/ismej.2009.44

Boynton, W. R., Kemp, W. M., Osborne, C. G., Kaumeyer, K. R., & Jenkins, M. C. (1981). Influence of water circulation rate on in situ measurements of benthic community respiration. *Marine Biology*, *65*(2), 185–190. https://doi.org/10.1007/BF00397084

Bricker-Urso, S., Nixon, S. W., Cochran, J. K., Hirschberg, D. J., & Hunt, C. (1989). Accretion rates and sediment accumulation in Rhode Island salt marshes. *Estuaries*, *12*(4), 300. https://doi.org/10.2307/1351908

Bulseco, A. N., Giblin, A. E., Tucker, J., Murphy, A. E., Sanderman, J., Hiller-Bittrolff, K., & Bowen, J. L. (2019). Nitrate addition stimulates microbial decomposition of organic matter in salt marsh sediments. *Global Change Biology*, *25*(10), 3224–3241. https://doi.org/10.1111/gcb.14726

Bulseco, A. N., Vineis, J. H., Murphy, A. E., Spivak, A. C., Giblin, A. E., Tucker, J., & Bowen, J. L. (2020). Metagenomics coupled with biogeochemical rates measurements provide evidence that nitrate addition stimulates respiration in salt marsh sediments. *Limnology & Oceanography*, *65*(S1), S321–S339. https://doi.org/10.1002/lno.11326

Burdick, D. M., & Mendelssohn, I. A. (1990). Relationship between anatomical and metabolic responses to soil waterlogging in the Coastal Grass Spartina patens. *Journal of Experimental Botany*, *41*(2), 223–228. https://doi.org/10.1093/jxb/41.2.223

Canuel, E. A., Freeman, K. H., & Wakeham, S. G. (1997). Isotopic compositions of lipid biomarker compounds in estuarine plants and surface sediments. *Limnology & Oceanography*, *42*(7), 1570–1583. https://doi.org/10.4319/lo.1997.42.7.1570

Canuel, E. A., & Martens, C. S. (1993). Seasonal variations in the sources and alteration of organic matter associated with recently-deposited sediments. *Organic Geochemistry*, *20*(5), 563–577. https://doi.org/10.1016/0146-6380(93)90024-6

Canuel, E. A., & Martens, C. S. (1996). Reactivity of recently deposited organic matter: Degradation of lipid compounds near the sediment-water interface. *Geochimica et Cosmochimica Acta*, *60*(10), 1793–1806. https://doi.org/10.1016/0016-7037(96)00045-2

Canuel, E. A., Spivak, A. C., Waterson, E. J., & Emmett Duffy, J. (2007). Biodiversity and food web structure influence short-term accumulation of sediment organic matter in an experimental seagrass system. *Limnology & Oceanography*, *52*(2), 590–602. https://doi.org/10.4319/lo.2007.52.2.0590

Cavatorta, J. R., Johnston, M., Hopkinson, C., & Valentine, V. (2003). Patterns of sedimentation in a salt marsh-dominated estuary. *The Biological Bulletin*, *205*(2), 239–241. https://doi.org/10.2307/1543274

Chambers, L. G., Steinmuller, H. E., & Breithaupt, J. L. (2019). Toward a mechanistic understanding of "peat collapse" and its potential contribution to coastal wetland loss. *Ecology*, *100*(7). https://doi.org/10.1002/ecy.2720

Chmura, G. L., Coffey, A., & Crago, R. (2001). Variation in surface sediment deposition on salt marshes in the Bay of Fundy. *Journal of Coastal Research*, *17*(1), 221–227.

Craft, C., Clough, J., Ehman, J., Joye, S., Park, R., Pennings, S., et al. (2009). Forecasting the effects of accelerated sea-level rise on tidal marsh ecosystem services. *Frontiers in Ecology and the Environment*, *7*(2), 73–78. https://doi.org/10.1890/070219

Day, J. W., Kemp, G. P., Reed, D. J., Cahoon, D. R., Boumans, R. M., Suhayda, J. M., & Gambrell, R. (2011). Vegetation death and rapid loss of surface elevation in two contrasting Mississippi delta salt marshes: The role of sedimentation, autocompaction and sea-level rise. *Ecological Engineering*, *37*(2), 229–240. https://doi.org/10.1016/j.ecoleng.2010.11.021

Deegan, L. A., Johnson, D. S., Warren, R. S., Peterson, B. J., Fleeger, J. W., Fagherazzi, S., & Wollheim, W. M. (2012). Coastal eutrophication as a driver of salt marsh loss. *Nature*, *490*(7420), 388–392. https://doi.org/10.1038/nature11533

DeLaune, R. D., Nyman, J. A., & Patrick, W. H., Jr. (1994). Peat collapse, ponding and wetland loss in a rapidly submerging coastal marsh. *Journal of Coastal Research*, *10*(4), 1021–1030.

FitzGerald, D. M., Hughes, Z. J., Georgiou, I. Y., Black, S., & Novak, A. (2020). Enhanced, climate-driven sedimentation on salt marshes. *Geophysical Research Letters*, *47*(10), e2019GL086737. https://doi.org/10.1029/2019GL086737

Fleurence, J., Gutbier, G., Mabeau, S., & Leray, C. (1994). Fatty acids from 11 marine macroalgae of the French Brittany coast. *Journal of Applied Phycology*, *6*(5–6), 527–532. https://doi.org/10.1007/BF02182406

Friedrichs, C. T., & Perry, J. E. (2001). Tidal salt marsh morphodynamics: A synthesis. *Journal of Coastal Research*, 7–37.

Ganju, N. K., Couvillion, B. R., Defne, Z., & Ackerman, K. V. (2022). Development and application of Landsat-based wetland vegetation cover and UnVegetated-vegetated marsh ratio (UVVR) for the conterminous United States. *Estuaries and Coasts*, *45*(7), 1861–1878. https://doi.org/10.1007/s12237-022-01081-x

Giblin, A. (2021). AmeriFlux BASE US-PHM Plum Island high marsh, ver. 3-5 [Dataset]. AmeriFlux AMP, https://doi.org/10.17190/AMF/1543377

Goñi, M. A., Thomas, K. A., & Goni, M. A. (2000). Sources and transformations of organic matter in surface soils and sediments from a tidal estuary (North Inlet, South Carolina, USA). *Estuaries*, *23*(4), 548. https://doi.org/10.2307/1353145

Gonneea, M. E., Maio, C. V., Kroeger, K. D., Hawkes, A. D., Mora, J., Sullivan, R., et al. (2019). Salt marsh ecosystem restructuring enhances elevation resilience and carbon storage during accelerating relative sea-level rise. *Estuarine, Coastal and Shelf Science*, *217*, 56–68. https://doi.org/10.1016/j.ecss.2018.11.003

Google. (2022). [Google maps of Plum Island ecosystem—LTER]. Retrieved from https://goo.gl/maps/DAGAtxVcAaaFhwfN9

Hartig, E. K., Gornitz, V., Kolker, A., Mushacke, F., & Fallon, D. (2002). Anthropogenic and climate-change impacts on salt marshes of Jamaica Bay, New York City. *Wetlands*, *22*(1), 71–89. https://doi.org/10.1672/0277-5212(2002)022[0071:AACCIO]2.0.CO;2

Hedges, J. I., & Stern, J. H. (1984). Carbon and nitrogen determinations of carbonate-containing solids 1. *Limnology & Oceanography*, *29*(3), 657–663. https://doi.org/10.4319/lo.1984.29.3.0657

Henninger, T. O., Froneman, P. W., Richoux, N. B., & Hodgson, A. N. (2009). The role of macrophytes as a refuge and food source for the estuarine isopod Exosphaeroma hylocoetes. *Estuarine, Coastal and Shelf Science*, *82*(2), 285–293. https://doi.org/10.1016/j.ecss.2009.01.017

Herbert, E. R., Windham-Myers, L., & Kirwan, M. L. (2021). Sea-level rise enhances carbon accumulation in United States tidal wetlands. *One Earth*, *4*(3), 425–433. https://doi.org/10.1016/j.oneear.2021.02.011

Himmelstein, J., Vinent, O. D., Temmerman, S., & Kirwan, M. L. (2021). Mechanisms of pond expansion in a rapidly submerging marsh. *Frontiers in Marine Science*, *8*. https://doi.org/10.3389/fmars.2021.704768

Holmquist, J. R., Windham-Myers, L., Bliss, N., Crooks, S., Morris, J. T., Megonigal, J. P., et al. (2018). Accuracy and precision of tidal wetland soil carbon mapping in the conterminous United States. *Scientific Reports*, *8*(1), 9478. https://doi.org/10.1038/s41598-018-26948-7

Hopkinson, C. S., Morris, J. T., Fagherazzi, S., Wollheim, W. M., & Raymond, P. A. (2018). Lateral marsh edge erosion as a source of sediments for vertical marsh accretion. *Journal of Geophysical Research: Biogeosciences*, *123*(8), 2444–2465. https://doi.org/10.1029/2017JG004358

Janik, L. J., Skjemstad, J. O., Shepherd, K. D., & Spouncer, L. R. (2007). The prediction of soil carbon fractions using mid-infrared-partial least square analysis. *Soil Research*, *45*(2), 73. https://doi.org/10.1071/SR06083

Jeffries, H. P. (1972). Fatty-acid ecology of a tidal Marsh 1. *Limnology & Oceanography*, *17*(3), 433–440. https://doi.org/10.4319/lo.1972.17.3.0433

Johnston, M. E., Cavatorta, J. R., Hopkinson, C. S., & Valentine, V. (2003). Importance of metabolism in the development of salt marsh ponds. *The Biological Bulletin*, *205*(2), 248–249. https://doi.org/10.2307/1543278

Kaneda, T. (1991). Iso- and anteiso-fatty acids in bacteria: Biosynthesis, function, and taxonomic significance. *Microbiological Reviews*, *55*(2), 288–302. https://doi.org/10.1128/mr.55.2.288-302.1991

Kearney, M. S., Grace, R. E., & Stevenson, J. C. (1988). Marsh loss in Nanticoke estuary, Chesapeake Bay. *Geographical Review*, *78*(2), 205. https://doi.org/10.2307/214178

Lehmann, J., Hansel, C. M., Kaiser, C., Kleber, M., Maher, K., Manzoni, S., et al. (2020). Persistence of soil organic carbon caused by functional complexity. *Nature Geoscience*, *13*(8), 529–534. https://doi.org/10.1038/s41561-020-0612-3

Lorrain, A., Savoye, N., Chauvaud, L., Paulet, Y.-M., & Naulet, N. (2003). Decarbonation and preservation method for the analysis of organic C and N contents and stable isotope ratios of low-carbonated suspended particulate material. *Analytica Chimica Acta*, *491*(2), 125–133. https://doi.org/10.1016/S0003-2670(03)00815-8

Luk, S. Y., Spivak, A. C., Eagle, M. J., & O'Keefe Suttles, J. A. (2020). Collection, analysis, and age-dating of sediment cores from a salt marsh platform and ponds in, Rowley, Massachusetts, in 2014–15: U.S. Geological survey data release. https://doi.org/10.5066/P9HIOWKT

Luk, S. Y., Todd-Brown, K., Eagle, M., McNichol, A. P., Sanderman, J., Gosselin, K., & Spivak, A. C. (2021). Soil organic carbon development and turnover in natural and disturbed salt marsh environments. *Geophysical Research Letters*, *48*(2), e2020GL090287. https://doi.org/10.1029/2020GL090287

Mariotti, G. (2016). Revisiting salt marsh resilience to sea level rise: Are ponds responsible for permanent land loss? *Journal of Geophysical Research: Earth Surface*, *121*(7), 1391–1407. https://doi.org/10.1002/2016JF003900

Mariotti, G., & Fagherazzi, S. (2013). Critical width of tidal flats triggers marsh collapse in the absence of sea-level rise. *Proceedings of the National Academy of Sciences of the United States of America*, *110*(14), 5353–5356. https://doi.org/10.1073/pnas.1219600110

Mariotti, G., Spivak, A. C., Luk, S. Y., Ceccherini, G., Tyrrell, M., & Gonneea, M. E. (2020). Modeling the spatial dynamics of marsh ponds in New England salt marshes. *Geomorphology*, *365*, 107262. https://doi.org/10.1016/j.geomorph.2020.107262

Mendelssohn, I. A., & McKee, K. L. (1988). *Spartina Alterniflora* die-back in Louisiana: Time-course investigation of soil waterlogging effects. *Journal of Ecology*, *76*(2), 509–521. https://doi.org/10.2307/2260609

Millette, T. L., Argow, B. A., Marcano, E., Hayward, C., Hopkinson, C. S., & Valentine, V. (2010). Salt marsh geomorphological analyses via integration of multitemporal multispectral remote sensing with LIDAR and GIS. *Journal of Coastal Research*, *265*, 809–816. https://doi.org/10.2112/JCOASTRES-D-09-00101.1

Mitchener, H., & Torfs, H. (1996). Erosion of mud/sand mixtures. *Coastal Engineering*, *29*(1–2), 1–25. https://doi.org/10.1016/S0378-3839(96)00002-6

Morris, J. T., Barber, D. C., Callaway, J. C., Chambers, R., Hagen, S. C., Hopkinson, C. S., et al. (2016). Contributions of organic and inorganic matter to sediment volume and accretion in tidal wetlands at steady state. *Earth's Future*, *4*(4), 110–121. https://doi.org/10.1002/2015EF000334

Morris, J. T., Sundareshwar, P. V., Nietch, C. T., Kjerfve, B., & Cahoon, D. R. (2002). Responses of coastal wetlands to rising sea level. *Ecology*, *83*(10), 2869–2877. https://doi.org/10.1890/0012-9658(2002)083[2869:ROCWTR]2.0.CO;2

Ortiz, A. C., Roy, S., & Edmonds, D. A. (2017). Land loss by pond expansion on the Mississippi River Delta plain. *Geophysical Research Letters*, *44*(8), 3635–3642. https://doi.org/10.1002/2017GL073079

Penland, S. (2002). Geologic classification of coastal land loss between 1932 and 1990 in the Mississippi River Delta plain. *Southeastern Louisiana'*, *52*, 799–807.

R Core Team. (2022). R: A language and environment for statistical computing. Retrieved from https://www.R-project.org

Reed, D. J. (1989). Patterns of sediment deposition in subsiding coastal salt marshes, Terrebonne Bay, Louisiana: The role of winter storms. *Estuaries*, *12*(4), 222. https://doi.org/10.2307/1351901

Rigaud, S., Deflandre, B., Maire, O., Bernard, G., Duchêne, J. C., Poirier, D., & Anschutz, P. (2018). Transient biogeochemistry in intertidal sediments: New insights from tidal pools in Zostera noltei meadows of Arcachon Bay (France). *Marine Chemistry*, *200*, 1–13. https://doi.org/10.1016/j.marchem.2018.02.002

Rosenheim, B. E., Day, M. B., Domack, E., Schrum, H., Benthien, A., & Hayes, J. M. (2008). Antarctic sediment chronology by programmed-temperature pyrolysis: Methodology and data treatment: Pyrolysis of Antarctic sediments. *Geochemistry, Geophysics, Geosystems*, *9*(4), Q04005. https://doi.org/10.1029/2007GC001816

Sanderman, J., & Grandy, A. S. (2019). Ramped thermal analysis for isolating biologically meaningful soil organic matter fractions with distinct residence times. *Soils and Biogeochemical Cycling*. Preprint. https://doi.org/10.5194/soil-2019-44

Sanderman, J., Krull, E., Kuhn, T., Hancock, G., McGowan, J., Maddern, T., et al. (2015). Deciphering sedimentary organic matter sources: Insights from radiocarbon measurements and NMR spectroscopy. *Limnology & Oceanography*, *60*(3), 739–753. https://doi.org/10.1002/lno.10064

Schepers, L., Kirwan, M., Guntenspergen, G., & Temmerman, S. (2017). Spatio-temporal development of vegetation die-off in a submerging coastal marsh: Spatio-temporal marsh die-off. *Limnology & Oceanography*, *62*(1), 137–150. https://doi.org/10.1002/lno.10381

Schuerch, M., Rapaglia, J., Liebetrau, V., Vafeidis, A., & Reise, K. (2012). Salt marsh accretion and storm tide variation: An example from a barrier Island in the North Sea. *Estuaries and Coasts*, *35*(2), 486–500. https://doi.org/10.1007/s12237-011-9461-z

Sessions, A. L. (2006). Seasonal changes in D/H fractionation accompanying lipid biosynthesis in *Spartina alterniflora*. *Geochimica et Cosmochimica Acta*, *70*(9), 2153–2162. https://doi.org/10.1016/j.gca.2006.02.003

Smith, J. A. M., & Pellew, M. (2021). Pond dynamics yield minimal net loss of vegetation cover across an unditched salt marsh landscape. *Estuaries and Coasts*, *44*(6), 1534–1546. https://doi.org/10.1007/s12237-020-00882-2

Spivak, A., & Ossolinski, J. (2016). Limited effects of nutrient enrichment on bacterial carbon sources in salt marsh tidal creek sediments. *Marine Ecology Progress Series*, *544*, 107–130. https://doi.org/10.3354/meps11587

Spivak, A. C. (2015). Benthic biogeochemical responses to changing estuary trophic state and nutrient availability: A paired field and mesocosm experiment approach: Trophic history alters benthic processes. *Limnology & Oceanography*, *60*(1), 3–21. https://doi.org/10.1002/lno.10001

Spivak, A. C. (2020a). *Bulk soil and elemental properties of marsh and infilled pond soils collected in 2014-2015 within Plum Island ecosystems LTER*. Biological and Chemical Oceanography Data Management Office (BCO-DMO). https://doi.org/10.26008/1912/bco-dmo.827298.1

Spivak, A. C. (2020b). *Fourier transform infrared spectroscopy raw spectra of soils collected in 2014–2015 within Plum Island ecosystems LTER*. Biological and Chemical Oceanography Data Management Office (BCO-DMO). https://doi.org/10.26008/1912/bco-dmo.827452.1

Spivak, A. C. (2020c). *Ramped pyrolysis oxidation (RPO) temperature and carbon dioxide evolved values of soils collected in 2014–2015 within Plum Island ecosystems LTER*. Biological and Chemical Oceanography Data Management Office (BCO-DMO).

Spivak, A. C. (2020d). *Ramped pyrolysis oxidation (RPO) C isotope values of soils collected in 2014–2015 within Plum Island ecosystems LTER*. Biological and Chemical Oceanography Data Management Office (BCO-DMO). https://doi.org/10.26008/1912/bco-dmo.827365.1

Spivak, A. C., Canuel, E. A., Duffy, J. E., & Richardson, J. P. (2007). Top-down and bottom-up controls on sediment organic matter composition in an experimental seagrass ecosystem. *Limnology & Oceanography*, *52*(6), 2595–2607. https://doi.org/10.4319/lo.2007.52.6.2595

Spivak, A. C., Denmark, A., Gosselin, K. M., & Sylva, S. P. (2020). Salt marsh pond biogeochemistry changes hourly-to-yearly but does not scale with dimensions or geospatial position. *Journal of Geophysical Research: Biogeosciences*, *125*(10), e2020JG005664. https://doi.org/10.1029/2020JG005664

Spivak, A. C., Gosselin, K., Howard, E., Mariotti, G., Forbrich, I., Stanley, R., & Sylva, S. P. (2017). Shallow ponds are heterogeneous habitats within a temperate salt marsh ecosystem. *Journal of Geophysical Research: Biogeosciences*, *122*(6), 1371–1384. https://doi.org/10.1002/2017JG003780

Spivak, A. C., Gosselin, K. M., & Sylva, S. P. (2018). Shallow ponds are biogeochemically distinct habitats in salt marsh ecosystems. *Limnology & Oceanography*, *63*(4), 1622–1642. https://doi.org/10.1002/lno.10797

Stevenson, J. C., Kearney, M. S., & Pendleton, E. C. (1985). Sedimentation and erosion in a Chesapeake Bay brackish marsh system. *Marine Geology*, *67*(3–4), 213–235. https://doi.org/10.1016/0025-3227(85)90093-3

Swart, D. H. (1974). *Offshore sediment transport and equilibrium profiles* (Vol. 131, pp. 1–217). Delft Hydraulics Laboratory.

Tanner, B. R., Uhle, M. E., Mora, C. I., Kelley, J. T., Schuneman, P. J., Lane, C. S., & Allen, E. S. (2010). Comparison of bulk and compound-specific $\delta^{13}C$ analyses and determination of carbon sources to salt marsh sediments using n-alkane distributions (Maine, USA). *Estuarine, Coastal and Shelf Science*, *86*(2), 283–291. https://doi.org/10.1016/j.ecss.2009.11.023

Turner, R. E., & Rao, Y. S. (1990). Relationships between wetland fragmentation and recent hydrologic changes in a deltaic coast. *Estuaries*, *13*(3), 272–281. https://doi.org/10.2307/1351918

Turner, R. E., Swenson, E. M., & Milan, C. S. (2002). Organic and inorganic contributions to vertical accretion in salt marsh sediments. In M. P. Weinstein & D. A. Kreeger (Eds.), *Concepts and controversies in tidal marsh ecology* (pp. 583–595). Kluwer Academic Publishers. https://doi.org/10.1007/0-306-47534-0_27

Viso, A.-C., & Marty, J.-C. (1993). Fatty acids from 28 marine microalgae. *Phytochemistry*, *34*(6), 1521–1533. https://doi.org/10.1016/S0031-9422(00)90839-2

Volkman, J. K., Jeffrey, S. W., Nichols, P. D., Rogers, G. I., & Garland, C. D. (1989). Fatty acid and lipid composition of 10 species of microalgae used in mariculture. *Journal of Experimental Marine Biology and Ecology*, *128*(3), 219–240. https://doi.org/10.1016/0022-0981(89)90029-4

Volkman, J. K., Johns, R. B., Gillan, F. T., Perry, G. J., & Bavor, H. J. (1980). Microbial lipids of an intertidal sediment—I. Fatty acids and hydrocarbons. *Geochimica et Cosmochimica Acta*, *44*(8), 1133–1143. https://doi.org/10.1016/0016-7037(80)90067-8

Walling, D. E., & Quine, T. A. (1994). Use of fallout radionuclide measurements in soil erosion investigations. *Proceedings of an international symposium held in Vienna* (pp. 17–21).

Wang, X.-C., Chen, R. F., & Berry, A. (2003). Sources and preservation of organic matter in Plum Island salt marsh sediments (MA, USA): Long-chain n-alkanes and stable carbon isotope compositions. *Estuarine, Coastal and Shelf Science*, *58*(4), 917–928. https://doi.org/10.1016/j.ecss.2003.07.006

Wiberg, P. L., & Sherwood, C. R. (2008). Calculating wave-generated bottom orbital velocities from surface-wave parameters. *Computers & Geosciences*, *34*(10), 1243–1262. https://doi.org/10.1016/j.cageo.2008.02.010

Williams, E. K., & Plante, A. F. (2018). A bioenergetic framework for assessing soil organic matter persistence. *Frontiers of Earth Science*, *6*, 143. https://doi.org/10.3389/feart.2018.00143

Williams, E. K., & Rosenheim, B. E. (2015). What happens to soil organic carbon as coastal marsh ecosystems change in response to increasing salinity? An exploration using ramped pyrolysis. *Geochemistry, Geophysics, Geosystems*, *16*(7), 2322–2335. https://doi.org/10.1002/2015GC005839

Wilson, B. J., Servais, S., Charles, S. P., Davis, S. E., Gaiser, E. E., Kominoski, J. S., et al. (2018). Declines in plant productivity drive carbon loss from brackish coastal wetland mesocosms exposed to saltwater intrusion. *Estuaries and Coasts*, *41*(8), 2147–2158. https://doi.org/10.1007/s12237-018-0438-z

Wilson, C. A., Hughes, Z. J., FitzGerald, D. M., Hopkinson, C. S., Valentine, V., & Kolker, A. S. (2014). Saltmarsh pool and tidal creek morphodynamics: Dynamic equilibrium of northern latitude saltmarshes? *Geomorphology*, *213*, 99–115. https://doi.org/10.1016/j.geomorph.2014.01.002

Wilson, K. R., Kelley, J. T., Croitoru, A., Dionne, M., Belknap, D. F., & Steneck, R. (2009). Stratigraphic and ecophysical characterizations of salt pools: Dynamic landforms of the Webhannet salt marsh, wells, ME, USA. *Estuaries and Coasts*, *32*(5), 855–870. https://doi.org/10.1007/s12237-009-9203-7

Wilson, K. R., Kelley, J. T., Tanner, B. R., & Belknap, D. F. (2010). Probing the Origins and Stratigraphic Signature of Salt Pools from North-Temperate Marshes in Maine, USA. *Journal of Coastal Research*, *26*, 1007–1026. https://doi.org/10.2112/JCOASTRES-D-10-00007.1

Yang, H., Yan, R., Chen, H., Zheng, C., Lee, D. H., & Liang, D. T. (2006). In-depth investigation of biomass pyrolysis based on three major components: Hemicellulose, cellulose and lignin. *Energy & Fuels*, *20*(1), 388–393. https://doi.org/10.1021/ef0580117

Young, I., & Verhagan, L. (1996). The growth of fetch limited waves in water of finite depth. Part 1: Total energy and peak frequency. *Coastal Engineering*, *27*(1–2), 47–78. https://doi.org/10.1016/S0378-3839(96)00006-3